Serum- and glucocorticoid-induced kinase 3 in recycling endosomes mediates acute activation of Na^+/H^+ exchanger NHE3 by glucocorticoids

Peijian He[a], Sei-Jung Lee[a], Songbai Lin[a], Ursula Seidler[b], Florian Lang[c], Geza Fejes-Toth[d], Aniko Naray-Fejes-Toth[d], and C. Chris Yun[a]

[a]Division of Digestive Diseases, Department of Medicine, Emory University, Atlanta, GA 30324; [b]Department of Gastroenterology, Hepatology, and Endocrinology, Hannover Medical School, 30625 Hannover, Germany; [c]Department of Physiology, Tubingen University, 72074 Tubingen, Germany; [d]Department of Physiology, Dartmouth Medical School, Lebanon, NH 03756

ABSTRACT **Na^+/H^+ exchanger 3 (NHE3) is the major Na^+ transporter in the intestine. Serum- and glucocorticoid-induced kinase (SGK) 1 interacts with NHE regulatory factor 2 (NHERF2) and mediates activation of NHE3 by dexamethasone (Dex) in cultured epithelial cells. In this study, we compared short-term regulation of NHE3 by Dex in SGK1-null and NHERF2-null mice. In comparison to wild-type mice, loss of SGK1 or NHERF2 significantly attenuated regulation of NHE3 by Dex but did not completely obliterate the effect. We show that transfection of SGK2 or SGK3 in PS120 cells resulted in robust activation of NHE3 by Dex. However, unlike SGK1 or SGK2, SGK3 rapidly activated NHE3 within 15 min of Dex treatment in both PS120 and Caco-2bbe cells. Immunofluorescence analysis showed that SGK3 colocalized with NHE3 in recycling endosomes, whereas SGK1 and SGK2 were diffusely distributed. Mutation of Arg-90 of SGK3 disrupted the endosomal localization of SGK3 and delayed NHE3 activation. Activation of SGK3 and NHE3 by Dex was dependent on phosphoinositide 3-kinase (PI3K) and phosphoinositide-dependent kinase 1 (PDK1), and Dex induced translocation of PDK1 to endosomes. Our study identifies SGK3 as a novel endosomal kinase that acutely regulates NHE3 in a PI3K-dependent mechanism.**

Monitoring Editor
M. Bishr Omary
University of Michigan

Received: Apr 18, 2011
Revised: Aug 8, 2011
Accepted: Aug 11, 2011

INTRODUCTION

Glucocorticoids (GCs) are widely used to treat inflammatory bowel disease (Campieri *et al.*, 1997). In addition to antiinflammatory effects, GCs show a direct effect on NaCl and water absorption in the intestine by targeting Na^+/H^+ exchanger 3 (NHE3; Charney *et al.*, 1975), which is the major Na^+ transporter located at the brush border membrane of the intestinal epithelium (He and Yun, 2010). Early studies showed that GCs stimulate NHE3 primarily through a genomic effect that increases NHE3 transcripts (Yun *et al.*, 1993). More recently, GCs were implicated in nongenomic regulation of NHE3, with GCs stimulating NHE3 activity without changing NHE3 expression levels, and serum- and glucocorticoid-induced kinase (SGK) 1 was subsequently shown to mediate nongenomic regulation of NHE3 by GCs (Baum *et al.*, 1994; Yun *et al.*, 2002a; Wang *et al.*, 2005, 2007).

SGK1 was initially identified by a differential screen of a rat mammary tumor cell line in search of GC-inducible genes (Webster *et al.*, 1993), and a subsequent protein sequence homology search identified two additional SGK isoforms, SGK2 and SGK3 (also known as cytokine-independent survival kinase; Kobayashi *et al.*, 1999). A body of evidence shows that SGKs share similar functions in regulation of a broad range of ion transporters and channels, including glutamate transporters (Boehmer *et al.*, 2003), Na^+ channels (Alvarez

This article was published online ahead of print in MBoC in Press (http://www.molbiolcell.org/cgi/doi/10.1091/mbc.E11-04-0328) on August 24, 2011.

Address correspondence to: C. Chris Yun (ccyun@emory.edu).

Abbreviations used: BCECF-AM, 2′,7′-bis-(2-carboxyethyl)-5-carboxyfluorescein acetoxymethyl ester; CMV, cytomegalovirus; Dex, dexamethasone; EGTA, ethylene glycol tetraacetic acid; GC, glucocorticoid, GFP, green fluorescent protein; GR, glucocorticoid receptor; HA, hemagglutinin; IBC, intrinsic buffering capacity; LY, PI3K inhibitor LY294002; NHE, Na+/H+ exchanger; NHERF2, NHE regulatory factor 2; OK, opossum kidney; PBS, phosphate-buffered saline; PDK1, phosphoinositide-dependent kinase 1; pH_i, intracellular pH; PI3K, phosphoinositide 3-kinase; PX, phox homology; RT-PCR, reverse transcription PCR; RU, RU486; SGK, serum- and glucocorticoid-induced kinase; shRNA, short-hairpin RNA; TMA-PO4, tetramethylammonium-PO4; TR-FRET, time-resolved fluorescence–fluorescence resonance energy transfer; VSVG, vesicular stomatitis virus glycoprotein; WGA, wheat germ agglutinin; WT, wild type.

de la Rosa *et al.*, 1999; Naray-Fejes-Toth *et al.*, 1999; Debonneville *et al.*, 2001; Friedrich *et al.*, 2003; Helms *et al.*, 2003), K^+ channels (Gamper *et al.*, 2002; Yun *et al.*, 2002b; Embark *et al.*, 2003), amino acid transporter (Bohmer *et al.*, 2010), and Na^+, K^+-ATPase (Henke *et al.*, 2002). However, it is noteworthy that these SGK isoforms differ in some aspects of their functions: SGK1 and SGK3, but not SGK2, stimulate the calcium channel TRPV5 (Embark *et al.*, 2004); SGK3, but not SGK1, mediates activation of glutamate receptor 1 and human ether-a-go-go channel (Maier *et al.*, 2006). SGK1 stimulates GluR6 (Strutz-Seebohm *et al.*, 2005b), whereas SGK3 stimulates GluR1 (Strutz-Seebohm *et al.*, 2005a). Furthermore, the phenotypes of mice deficient in SGK1 or SGK3 are distinct, clearly demonstrating nonredundant functions of the SGK proteins (Wulff *et al.*, 2002; McCormick *et al.*, 2004).

At the protein level, SGKs have 50% homology in their carboxyl-termini and only 15% homology in their NH_2-termini (Kobayashi *et al.*, 1999). In comparison to SGK1, SGK2 contains a relatively short NH_2-terminus, whereas SGK3 has a longer NH_2-terminus comprising a phox homology (PX) domain. The PX domain was originally found as a conserved domain in the $p40^{phox}$ and $p47^{phox}$ subunits of NADPH-oxidase complex (Ponting, 1996). The PX domain binds phosphoinositide, and it is present in many proteins involved in intracellular trafficking, such as sorting nexins (Worby and Dixon, 2002). In the case of SGK3, studies have shown that the PX domain is essential for targeting SGK3 to endosomes (Jun *et al.*, 2001; Virbasius *et al.*, 2001; Tessier and Woodgett, 2006), and this PX-dependent endosomal targeting results in distinct subcellular localization of SGK3 relative to SGK1 and SGK2. Interestingly, NHE3 resides in the endosomal compartment, which constitutes a major part of NHE3 regulation (Biemesderfer *et al.*, 1997; D'Souza *et al.*, 1998; Kurashima *et al.*, 1998), raising the possibility that SGK3 colocalizes with NHE3 in the same endosomal compartments.

In cultured epithelial cells, we have shown previously that SGK1 acutely regulates NHE3 activity, and this regulation requires the presence of NHE regulatory protein 2 (NHERF2), which tethers NHE3 and SGK1 to facilitate phosphorylation of NHE3 by SGK1 (Yun *et al.*, 2002a; Wang *et al.*, 2005, 2007). The importance of SGK1 in regulation of NHE3 is supported by the report that dexamethasone (Dex)-induced activation of NHE3 is significantly compromised in SGK1-null intestine (Grahammer *et al.*, 2006). However, animals were treated for 4 d with Dex in the former study, and whether short-term regulation of NHE3 is also perturbed has not been determined. In the current study, we investigated the effects of short-term Dex treatment on NHE3 activity in SGK1-null and NHERF2-null intestine. Additionally, we show that SGK3 colocalized with NHE3 in recycling endosomes acutely stimulates NHE3, providing a new insight into the role of SGK3 and acute regulation of NHE3.

RESULTS

SGK1 and NHERF2 play important roles in Dex-mediated stimulation of NHE3 in ileum

It was shown previously that treatment of SGK1-null mice with Dex for 96 h resulted in an ~40% increase in NHE3 activity compared with ~110% in wild-type (WT) mice (Grahammer *et al.*, 2006). For the current study, we mated $Sgk1^{flox/flox}$ mice with *Villin-Cre* mice to generate $Sgk1^{flox/flox}$*;Villin-Cre* mice, in which the *Villin* promoter directs the deletion of *Sgk1* gene in the epithelial cells in the intestine (Pinto *et al.*, 1999). The expression of SGK1 was examined by reverse transcription PCR (RT-PCR) and Western blotting to confirm the absence of SGK1 in the intestinal epithelial cells of $Sgk1^{flox/flox}$*;Villin-Cre* mice (Supplementary Figure S1, A and B).

Because our initial proposal for the role of SGK1 in NHE3 regulation pertains to short-term rather than chronic regulation (Grahammer *et al.*, 2006), we investigated the effects of Dex treatment for 4 h as a short-term treatment and 24 h as a long-term treatment. The basal rate of Na^+-dependent pH change by NHE3 measured in the presence of NHE1 and NHE2 inhibitor Hoe-694 in isolated villi of $Sgk1^{flox/flox}$ and $Sgk1^{flox/flox}$*;Villin-Cre* mice was not changed by the loss of SGK1 (Figure 1). Dex treatment of $Sgk1^{flox/flox}$ mice for 4 and 24 h increased NHE3 activity in the ileum by ~120% (Figure 1, A and B). In contrast, the loss of SGK1 in $Sgk1^{flox/flox}$*;Villin-Cre* mice markedly decreased the effect of Dex resulting in only ~25–30% increase in NHE3 activity (Figure 1, C and D). These findings reveal that SGK1 plays a significant role in, but is not obligatory for, Dex-mediated stimulation of NHE3. To ensure that the remaining increase in Na^+-dependent pH change in $Sgk1^{flox/flox}$*;Villin-Cre* ileal epithelial cells is due to NHE3 activity, Na^+-dependent pH recovery was measured in the presence of the NHE3 inhibitor S-3226. Our results showed that the Hoe-694-insensitive Na^+/H^+ exchange activity was ablated by S-3226 (Supplementary Figure S2, A and B), confirming its NHE3 origin.

We have shown previously that NHERF2 is necessary for SGK1-dependent regulation of NHE3 (Yun *et al.*, 2002a). To determine the role of NHERF2 in vivo, we examined the effects of Dex treatment for 4 and 24 h in isolated villi of $Nherf2^{-/-}$ mice. Immunoblotting confirmed that NHERF2 is absent in the mucosa of $Nherf2^{-/-}$ mice intestine, and that the expression level of SGK1 is not changed in $Nherf2^{-/-}$ mice (Supplementary Figure S1B). As for $Sgk1^{flox/flox}$*;Villin-Cre* villi, the loss of NHERF2 resulted in ~30% and ~45% increases at 4 and 24 h, respectively, compared with ~120% in WT villi (Figure 1, E and F). These studies show that SGK1 and NHERF2 are needed for the activation of NHE3 activity by Dex at 4 and 24 h, which is consistent with previous studies using cultured cells. However, the residual activation of NHE3 in the absence of SGK1 or NHERF2 suggests that additional means for NHE3 activation must be present (Yun *et al.*, 2002a). One potential mechanism involves increased NHE3 expression, but our earlier study showed that NHE3 protein abundance does not change at 4 h (Wang *et al.*, 2007), requiring an alternative explanation.

Differential regulation of NHE3 by SGK1, SGK2, and SGK3

Because other SGK isoforms, SGK2 and SGK3, can mediate similar effects, we sought to determine whether SGK2 or SGK3 regulates NHE3 activity in response to Dex treatment. The presence of SGK2 and SGK3 in small intestine was confirmed by RT-PCR. The expression levels of SGK2 and SGK3 mRNA in intestinal epithelial cells were not changed by the loss of SGK1 in $Sgk1^{flox/flox}$*;Villin-Cre* mice (Supplementary Figure S1A). PS120 cells stably expressing rabbit NHE3 with a vesicular stomatitis virus glycoprotein (VSVG) epitope fused at the carboxyl-terminus, PS120/NHE3V, were transfected with hemagglutinin (HA)-SGK1, -SGK2, or -SGK3, and the resulting cells were treated with 1 μM Dex (Figure 2A). Overexpression of SGK1 did not mediate an apparent activation of NHE3 by Dex, as PS120 cells lacked NHERF2 expression (Figure 2B), which is required for SGK1-mediated NHE3 regulation (Yun *et al.*, 2002a). In contrast, both SGK2 and SGK3 showed significant increases in NHE3 activity at both 4 and 24 h of Dex treatment (Figure 2, C and D), suggesting that the remaining NHE3 activation in $Sgk1^{flox/flox}$*;Villin-Cre* mice might have been due to the activities of SGK2 and SGK3. Surprisingly, Dex treatment showed a marked increase in NHE3 activity in PS120/NHE3V/HA-SGK3 cells at 15 min (Figure 2D), but not in cells expressing SGK1 or SGK2. To our knowledge, this is the first observation of such a rapid effect by Dex on NHE3. However, we did not observe any effect at 5 min, and we considered 15 min as the earliest time needed for Dex to regulate NHE3.

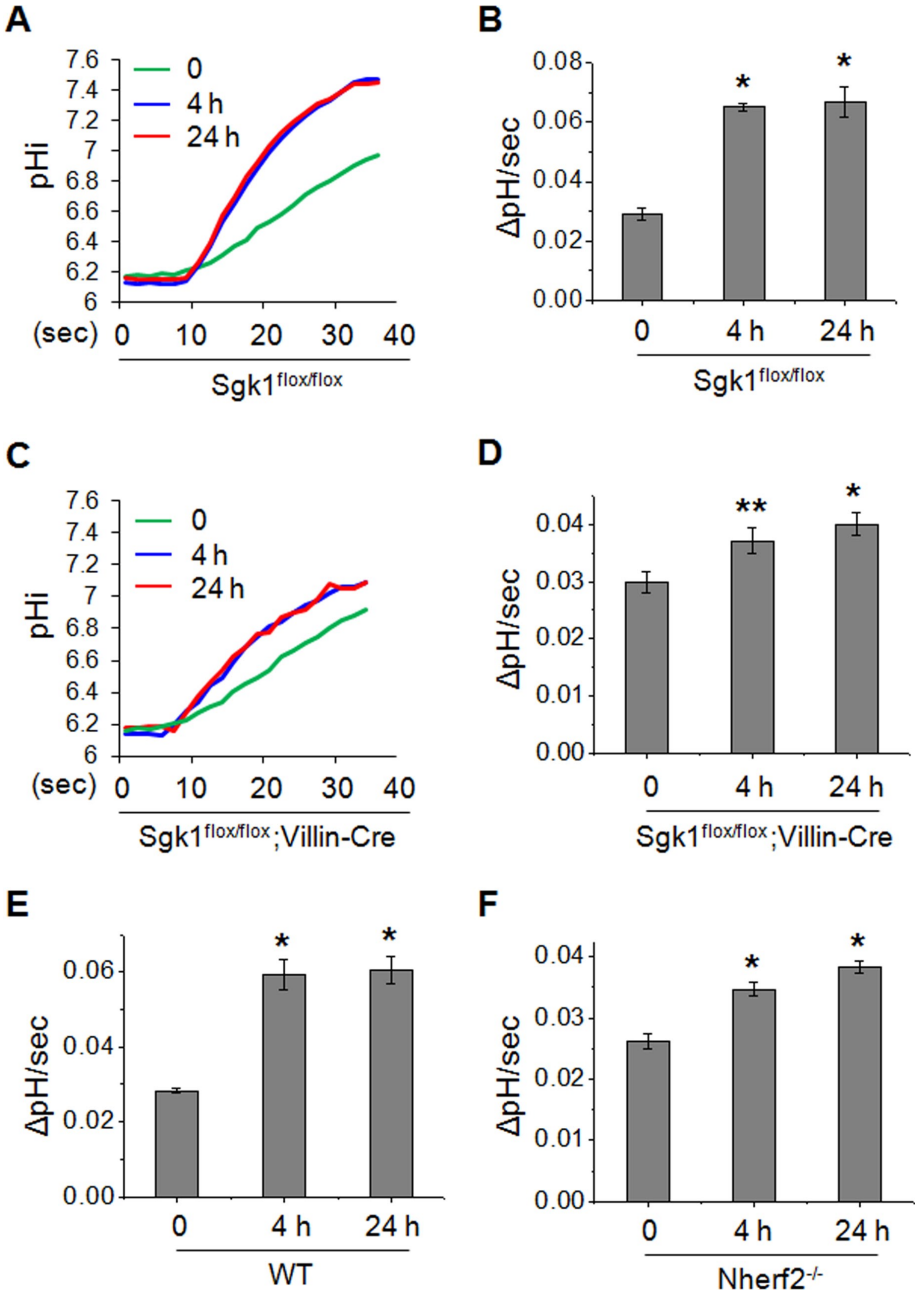

FIGURE 1: SGK1 and NHERF2 play important roles in Dex-induced activation of NHE3 in mouse ileum. Mice were injected intraperitoneally with Dex at 2 mg/kg body weight. After 4 or 24 h, villi were isolated from the ileum and NHE3 activity was measured in the presence of 50 μM Hoe-694 (NHE1 and NHE2 inhibitor). Increased rates of pH recovery following 4 or 24 h of Dex treatment were observed. (A) Representative traces of Na^+-dependent pH recovery in *Sgk1*$^{flox/flox}$ mice are shown. (B) NHE3 activities in *Sgk1*$^{flox/flox}$ villi are presented as the rate of Na^+-dependent pH change by determining $\Delta pH_i/\Delta time$ at pH_i 6.5 using typical traces shown in (A). NHE3 activities are shown as mean ± SE. (C) Representative traces of Na^+-dependent pH recovery in the ileal villi prepared from *Sgk1*$^{flox/flox}$*;Villin-Cre* mice are shown. (D) NHE3 activities in *Sgk1*$^{flox/flox}$*;Villin-Cre* villi are presented as the rate of Na^+-dependent pH change at pH_i 6.5. Stimulation of NHE3-dependent pH recovery is significantly attenuated in *Sgk1*$^{flox/flox}$*;Villin-Cre* mice compared with *Sgk1*$^{flox/flox}$ mice. NHE3 activities at pH_i 6.5 are shown in (E) WT and (F) *Nherf2*$^{-/-}$ mice. For all experiments, n = 3–4 mice and 6–8 villi per mouse were used. *, $p < 0.01$ and **, $p < 0.05$, compared with the untreated control.

In light of our unexpected findings, we examined whether Dex acutely regulates NHE3 in vivo. Because 15-min treatment of animals in vivo is not feasible, isolated villi were treated with 1 μM Dex ex vivo for 15 min prior to measurement of NHE3 activity. Intriguingly, NHE3 activity was significantly increased (~25%) in *Sgk1*$^{flox/flox}$ mice (Figure 3A), validating the acute regulation of NHE3 by Dex. Moreover, Dex stimulated NHE3 activity in both *Sgk1*$^{flox/flox}$*;Villin-Cre* and *Nherf2*$^{-/-}$ villi to the same extent as WT villi (Figure 3, A and B), further demonstrating that Dex-induced acute (15 min) stimulation of NHE3 in the intestine is independent of SGK1 and NHERF2. We confirmed that the acute pH recovery was due to NHE3 by using S-3226 (Supplementary Figure S2C).

Differential regulation of SGK1, SGK2, and SGK3 kinase activity by Dex

Despite the similarity in SGK isoforms, SGK1 is the only isoform for which expression is regulated by GCs. However, there is the possibility that Dex treatment regulates the kinase activity without a change in the expression level. Therefore we examined whether the kinase activity of these SGKs is regulated by Dex. We again used PS120/NHE3V cells expressing HA-SGK1, HA-SGK2 or HA-SGK3 to determine the effect of Dex on SGK kinase activity. These cells have an advantage in that the expression of SGKs is under the control of cytomegalovirus (CMV) promoter and is not altered by Dex. Cells were treated with Dex for 0–24 h, and HA-SGKs were immunoprecipitated with anti-HA antibodies. The amounts of SGKs were normalized by Western immunoblot analysis of an aliquot of immunoprecipitated proteins to ensure that the identical amount of SGK protein was used in the kinase assay. We determined SGK kinase activity by two approaches: by using [γ-^{32}P]ATP and by a nonradioisotope time-resolved fluorescence–fluorescence resonance energy transfer (TR-FRET) method. Figure 4 shows that the kinase activities of SGK1, SGK2, and SGK3 were similarly increased at 4 and 24 h of Dex treatment. However, unlike that of SGK1 or SGK2 (Figure 4, A and B), SGK3 activity was markedly increased at 15 min (Figure 4C). The nonradioactive TR-FRET assay yielded similar results (Supplementary Figure S3). Although the extent of increases was smaller in the TR-FRET assay, it is important to note that the results were qualitatively identical to [γ-^{32}P]-labeling of Crosstide. We therefore used the TR-FRET method to determine kinase activity in the subsequent experiments.

SGK2 and SGK3 mediate exocytotic trafficking and phosphorylation of NHE3

We showed previously that SGK1 stimulates NHE3 activity by increasing NHE3 expression at the cell surface (Wang *et al.*, 2005). To

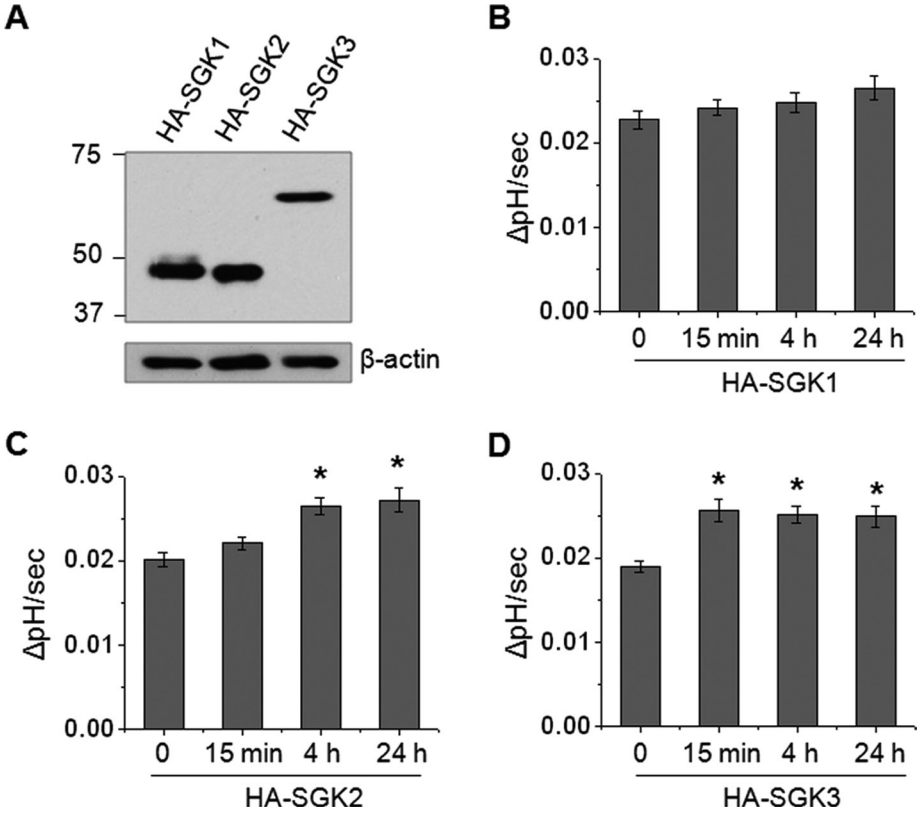

FIGURE 2: SGK3 rapidly activates NHE3 in response to Dex. (A) PS120/NHE3V cells were stably transfected with HA-SGK1, HA-SGK2, and HA-SGK3, and the expression levels of SGKs were determined by immunoblotting using an anti-HA antibody. Western blot of β-actin was used as loading control. PS120/NHE3V cells expressing (B) HA-SGK1, (C) HA-SGK2, or (D) HA-SGK3 were treated with 1 μM Dex for t = 0, 15 min, 4 h, or 24 h, followed by determination of NHE3 activity. The rates of pH recovery at pH_i 6.7 are shown. n = 8. *, $p < 0.01$ compared with the untreated control.

determine whether SGK2 and SGK3 similarly increase NHE3 expression in the plasma membrane, we performed a surface biotinylation assay. Surface NHE3 abundance was significantly increased at 4 h of Dex treatment in SGK2-expressing cells, but no change at 15 min was observed (Figure 5A). In contrast, the presence of SGK3 resulted in a significant increase in surface NHE3 at both 15 min and 4 h of Dex treatment (Figure 5A).

We have previously shown that SGK1-mediated activation of NHE3 is dependent on phosphorylation of NHE3 at S663 (Wang *et al.*, 2005). Because SGK2 and SGK3 recognize the same phosphorylation motif (Kobayashi *et al.*, 1999), we sought to determine the importance of S663 in NHE3 regulation by SGK2 or SGK3. PS120/opossum NHE3 (OKNHE3) and PS120/OKNHE3-S663A (OKNHE3 with a mutation of serine 663 to alanine) cells transfected with HA-SGK2 or HA-SGK3 were treated with Dex. Dex treatment for 4 h stimulated the activity of NHE3 as we have shown earlier, but the mutation of S663A ablated the effect (Figure 5B). For SGK3, we treated the cells for 15 min, but as for SGK2, NHE3-S663A did not respond to Dex treatment (Figure 5C). Although direct phosphorylation of NHE3 by SGK2 or SGK3 was not shown here, the results demonstrate that the presence of S663 is required for NHE3 regulation by SGK2 and SGK3.

SGK3 and NHE3 colocalize in recycling endosomes

We then asked whether the distinct response of NHE3 to SGK3 could be related to their spatial localizations. Immunofluorescence analysis of PS120/NHE3V cells (Figure 6A, top and middle) showed that both SGK1 (green) and SGK2 (green) were diffusely expressed throughout the cells. SGK1 and SGK2 partially colocalized with NHE3 (red) based on the overlap of fluorescence labels but did not show any distinct compartmentalization with NHE3. In contrast, SGK3 labeling showed localization in endosome-like compartments (Figure 6A, bottom) and, importantly, SGK3 (green) colocalized with NHE3 (red) in these vesicles. The endosomal location of SGK3 was confirmed by costaining with Rab5 (Figure 6B, bottom, red), an early endosome marker In contrast, neither SGK1 nor SGK2 colocalized with Rab5 in early endosomes (Figure 6B, top and middle). Furthermore, we examined whether the SGKs are expressed in recycling endosomes. PS120/NHE3V cells were transfected with green fluorescent protein (GFP)-Rab11 (a marker for recycling endosome) together with FLAG-tagged SGK1, SGK2, or SGK3. Figure 6C shows that SGK1 and SGK2 (red) were not found in recycling endosomes where Rab11 (green) is expressed. In contrast, SGK3 (red) and NHE3 (blue) colocalized with Rab11 (green) in recycling endosomes (Figure 6D).

We next examined whether the endosomal localization of SGK3 is important for acute NHE3 regulation. It was shown that

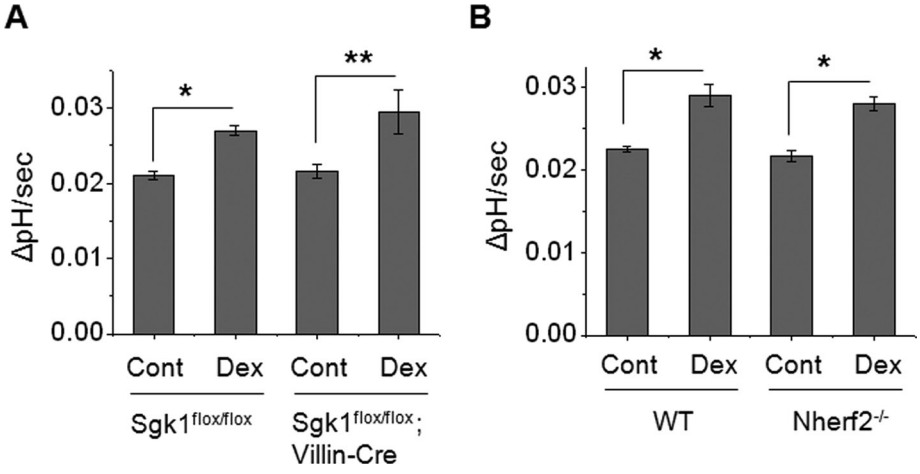

FIGURE 3: Dex acutely activates NHE3 in mouse intestine lacking SGK1 or NHERF2. (A) Villi were isolated from the *Sgk1*$^{flox/flox}$ and *Sgk1*$^{flox/flox}$*;Villin-Cre* ilea and were treated ex vivo with 1 μM Dex or carrier for 15 min prior to measurement of NHE3 activity in the presence of Hoe-694. The rates of pH recovery at pH_i 6.6 are shown. (B) The rates of pH recovery at pH_i 6.6 in WT and *Nherf2*$^{-/-}$ ilea treated with Dex for 15 min are shown. For all experiments, n = 3 mice and six villi per mouse were used. *, $p < 0.01$ and **, $p < 0.05$, compared with the control.

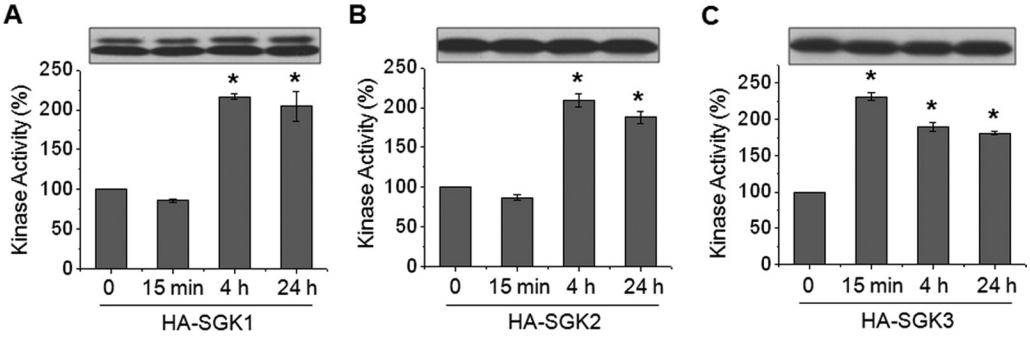

FIGURE 4: SGK3 kinase activity is acutely stimulated by Dex. PS120/NHE3V cells expressing HA-SGK1, HA-SGK2, or HA-SGK3 were treated with 1 μM Dex for t = 0, 15 min, 4 h, or 24 h. SGK proteins were purified by immunoprecipitation with an anti-HA antibody. To ensure the equal loading of immunoprecipitated SGKs, an aliquot of eluted protein was subjected to Western blotting using anti-HA antibody. Equal amounts of each SGK protein were used for in vitro kinase assay by using [γ-^{32}P]ATP, as detailed in *Materials and Methods*. The activities of (A) SGK1, (B) SGK2, and (C) SGK3 are shown relative to the basal SGK activity. n = 3. *, $p < 0.01$ compared with the untreated control.

the PX domain of SGK3 is critical for its endosomal localization, and mutation of R90 located in the PX domain disrupts the endosomal localization of SGK3 (Tessier and Woodgett, 2006). Therefore we expressed SGK3 or SGK3-R90A (SGK3 containing a mutation of Arg90 to Ala) in PS120/NHE3V cells (Figure 7A). Immunofluorescence staining confirmed that the R90A mutation perturbed the cellular location of SGK3 and, unlike WT SGK3, the SGK3-R90A mutant diffusely expressed throughout the cytoplasm, which appears similar to the expression patterns of SGK1 and SGK2; consequently, SGK3-R90A did not colocalize with NHE3 (Figure 7B). Intriguingly, the effect of the R90A mutation on endosomal localization of SGK3 was also extended to regulation of its activity in response to Dex. The kinase activity of SGK3-R90A was elevated at 4 and 24 h, but not at 15 min, of Dex treatment (Figure 7C), suggesting that the acute regulation of SGK3 by Dex is related to the endosomal localization of SGK3. Moreover, SGK3-R90A failed to activate NHE3 activity at 15 min, but its effect was delayed until 4 h of Dex treatment (Figure 7D). These findings indicate that endosomal localization enables SGK3 to acutely regulate NHE3.

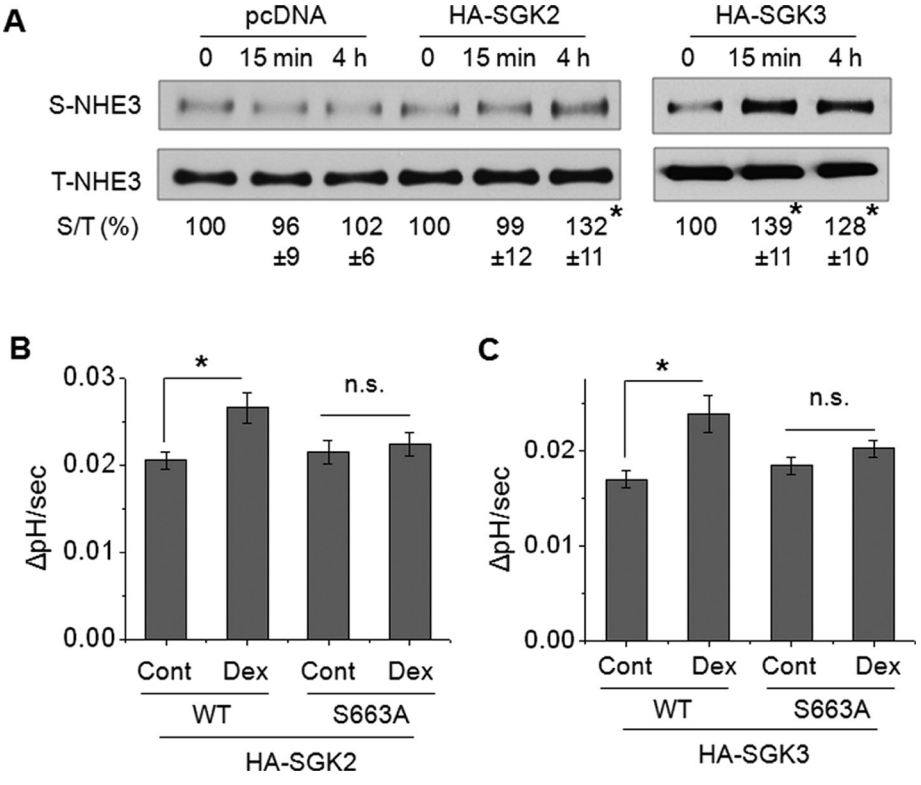

FIGURE 5: SGK2 and SGK3 increase NHE3 surface expression and the S663A mutation blocks the activation. (A) PS120/NHE3V/pcDNA, PS120/NHE3V/HA-SGK2, and PS120/NHE3V/HA-SGK3 cells were treated with 1 μM Dex for t = 0, 15 min, or 4 h, and the amount of NHE3 protein on the plasma membrane was determined by surface biotinylation, as detailed in *Materials and Methods*. The amount of surface (S) NHE3 was normalized to total (T) NHE3, and relative changes (%) are shown below the Western blots. n ≥ 3. (B) PS120/OKNHE3/HA-SGK2 and PS120/OKNHE3-S663A/HA-SGK2 cells were treated with 1 μM Dex for 4 h and NHE3 activity was measured. The rates of pH recovery at pH_i 6.8 are shown. n = 6. (C) PS120/OKNHE3/HA-SGK3 and PS120/OKNHE3-S663A/HA-SGK3 cells were treated with 1 μM Dex for 15 min, and NHE3 activity was determined. The rates of pH recovery at pH_i 6.8 are shown. n = 6. n.s., not significant. *, $p < 0.01$, compared with the untreated control.

SGK3-mediated activation of NHE3 is dependent on GR, phosphoinositide 3-kinase, and phosphoinositide-dependent kinase 1

Recent evidence has emphasized the short-term effects of GCs, but the mechanism of how GCs exert acute effects is incompletely understood. The presence of a G protein–coupled GC receptor (GR) that is insensitive to the GR antagonist, RU486 (RU), has been proposed (Maier *et al.*, 2005). Hence we first examined whether RU-insensitive GR is involved in the acute regulation of SGK3 by Dex. The preincubation of PS120/NHE3V/HA-SGK3 cells with RU (1 μM) did not affect the basal SGK3 activity but completely abrogated the Dex-induced rapid effect on SGK3 activity, suggesting the conventional GR and not the membrane-bound GR regulates SGK3 (Figure 8A). SGKs are related to Akt and are regulated by phosphoinositide 3-kinase (PI3K) and phosphoinositide-dependent kinase 1 (PDK1; Kobayashi *et al.*,

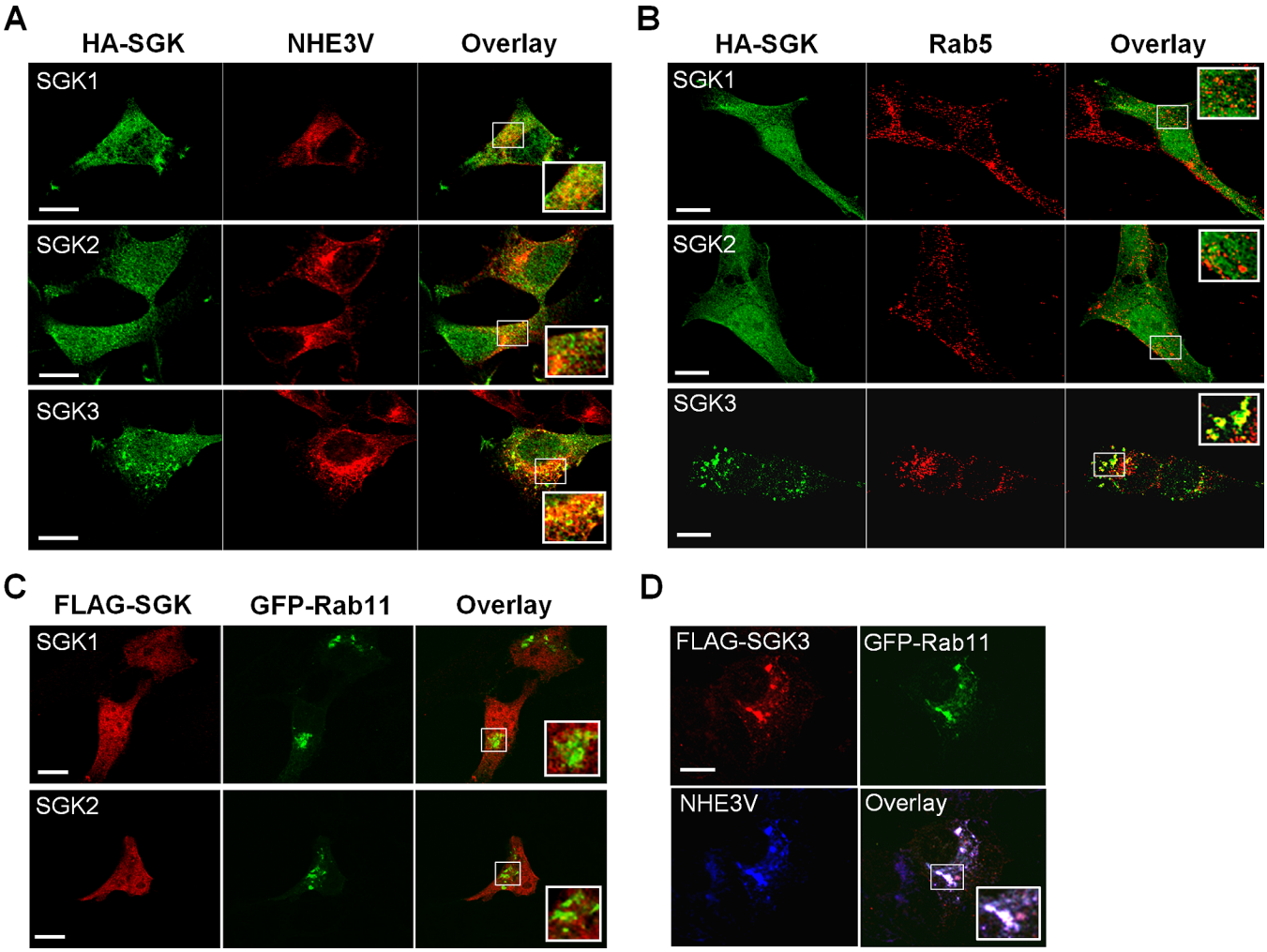

FIGURE 6: SGK3 colocalizes with NHE3 in recycling endosomes. (A) Cellular distribution of HA-tagged SGK1-3 (green) and NHE3V (red) in PS120 cells was determined by indirect immunofluorescence with anti-HA and anti-VSVG antibodies, respectively. The inset shows a magnified image of the boxed area. (B) Cellular localization of HA-tagged SGK1-3 (green) and Rab5 (red) in PS120 cells was determined with anti-HA and anti-Rab5 antibodies, respectively. (C) PS120/NHE3V cells were transfected with FLAG-tagged SGK1 or SGK2 and GFP-Rab11. The colocalization of SGK1 or SGK2 with Rab11 was determined with anti-FLAG antibody. (D) PS120/NHE3V cells were transfected with FLAG-SGK3 and GFP-Rab11. The colocalization of SGK3 (red) and NHE3V (blue) with GFP-Rab11 (green) was determined with anti-FLAG and anti-VSVG antibodies, respectively. Scale bar: 10 μm.

1999; Park *et al.*, 1999). In addition, it was shown that Dex stimulates PI3K activity by potentiating binding of GR to the p85 subunit of PI3K (Hafezi-Moghadam *et al.*, 2002). Hence we tested the involvement of PI3K by using the PI3K inhibitor, LY294002 (LY). Pretreatment with LY (20 μM) completely blocked the activation of SGK3 activity by 15 min of Dex treatment (Figure 8A). Similarly, RNA interference of PDK1 by short-hairpin RNA (shRNA), which reduced the PDK1 expression by ~70% (Figure 8B), ablated the stimulatory effect of Dex on SGK3 activity (Figure 8C). Consistent with the inhibition of SGK3 kinase activity, the acute regulation of NHE3 transport activity by Dex in SGK3-expressing cells was completely blocked when cells were pretreated with RU or LY (Figure 8D), or with knockdown of PDK1 (Figure 8E). Taken together, these data show that acute activation of SGK3 and NHE3 by Dex is through the GR-PI3K-PDK1 pathway. Because the effects of SGK2 and SGK3 on NHE3 at a later time point (4 h) are similar, we determined whether the delayed regulation of NHE3 by SGK2 and SGK3 is also dependent on PDK1. Knockdown of PDK1 ablated activation of NHE3 activity in cells expressing SGK2 or SGK3 (Supplementary Figure S4), suggesting that the Dex-induced PI3K-PDK1 pathway is not specific for acute (15 min) NHE3 activation by SGK3. We did not examine the role of PDK1 for SGK1 in PS120 cells, since SGK1 showed no effect on NHE3 (Figure 2B) unless NHERF2 was coexpressed, but we showed previously that regulation of NHE3 by SGK1 is PI3K-dependent (Yun *et al.*, 2002a).

If PDK1 is important for both SGK2- and SGK3-dependent regulation of NHE3, what allows the acute regulation of SGK3? To delineate the role of PDK1 in the rapid activation of SGK3 and NHE3, we examined the temporospatial location of phosphorylation of PDK1 (p-PDK1: an active form of PDK1 kinase) at Ser241 relative to SGK3 in response to Dex treatment. Fluorescence labeling of SGK3 (Figure 8F, green) partially colocalized with p-PDK1 (Figure 8F, red) under basal conditions, whereas treatment with Dex for 15 min resulted in increased overlap of their fluorescence labels (Figure 8F). A quantitative determination of colocalization of SGK1 and p-PDK1 showed a significant increase in colocalization coefficient induced by Dex treatment (Figure 8G). An *x,z* scan shows that Dex also increased colocalization of p-PDK1 and SGK3

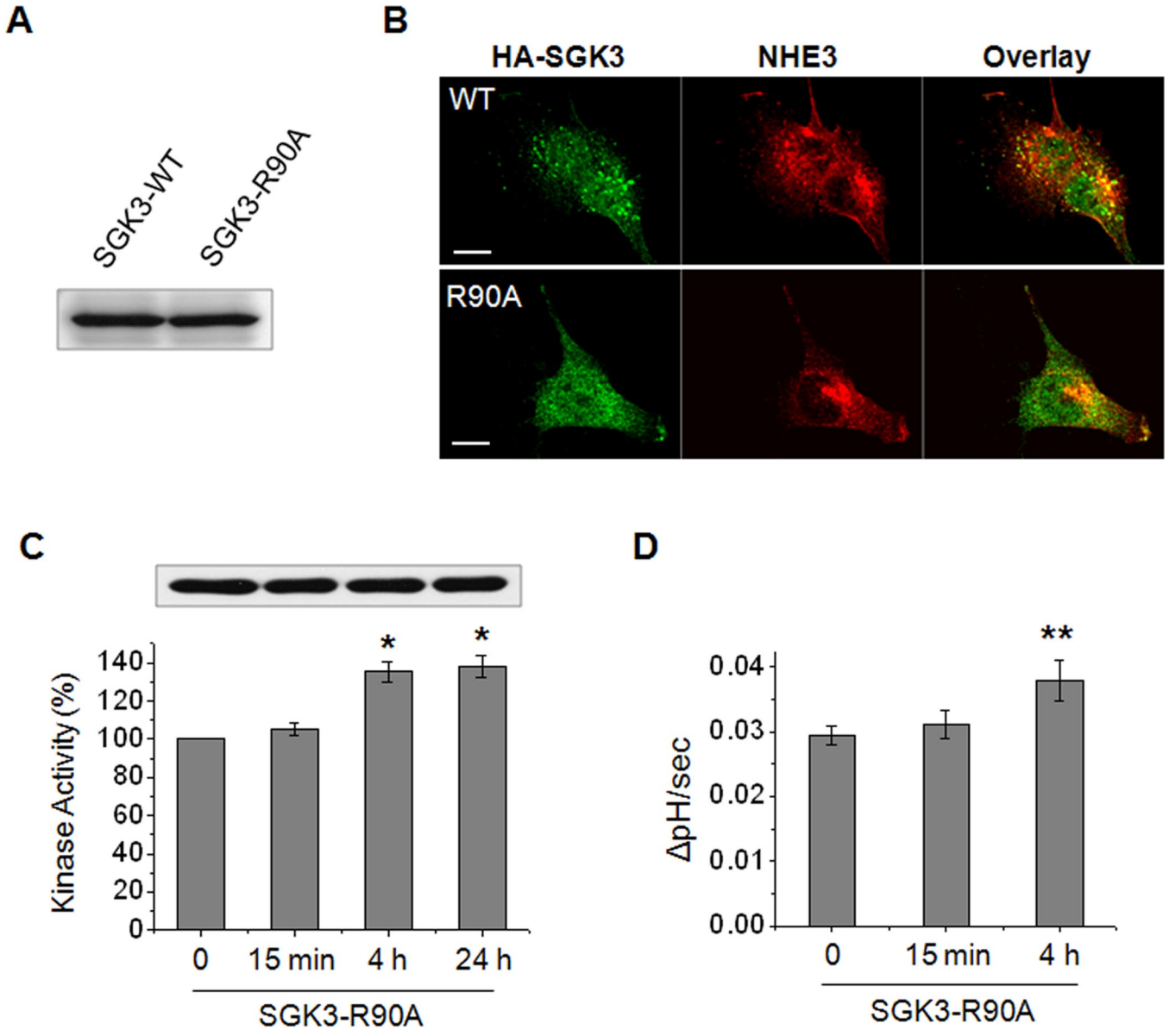

FIGURE 7: Acute regulation of NHE3 by SGK3 is dependent on the endosomal localization of SGK3. (A) PS120/NHE3V cells were expressed with HA-SGK3 or HA-SGK3-R90A, and the expression levels of SGK3 and SGK3-R90A in PS120/NHE3V cells were examined with anti-HA antibody. (B) Cellular distribution of SGK3 (green) or SGK3-R90A (green) with NHE3 (red) in PS120 cells was examined with anti-HA and anti-VSVG antibodies, respectively. Scale bar: 10 μm. (C) PS120/NHE3V/HA-SGK3-R90A cells were treated with Dex for t = 0, 15 min, 4 h, or 24 h, and SGK3-R90A protein was purified by immunoprecipitation for kinase assay. The kinase activities of SGK3-R90A are shown relative to the basal activity. n = 3. (D) PS120/NHE3V/HA-SGK3-R90A cells were treated with 1 μM Dex for t = 0, 15 min, or 4 h, followed by measurement of NHE3 activity. The rates of pH recovery at pH_i 6.7 are shown. n = 6. *, $p < 0.01$ and **, $p < 0.05$, compared with the untreated control.

in the perimembrane areas (Supplementary Figure S5). To determine whether Dex mobilizes p-PDK1 to endosomal compartments, we determined the expression patterns of p-PDK1(red) in GFP-Rab11 (green) upon 15 min of Dex treatment (Figure 8, H and I). The results show that the expression of p-PDK1 in recycling endosomes increased following Dex treatment. We also examined whether Dex-induced mobilization of p-PDK1 occurs in intestinal epithelial cells. Consistent with the findings in PS120 cells, Dex increased p-PDK1 expression in recycling endosomes in the human intestinal epithelial Caco-2bbe cells (Supplementary Figure S6). These findings demonstrate that Dex acutely activates NHE3 by mobilizing PDK1 to endosomal compartments in the cytoplasm and on the membrane, where it activates SGK3 that in turn phosphorylates NHE3.

SGK3 mediates acute activation of NHE3 in Caco-2bbe epithelial cells

To reproduce the regulation of NHE3 via SGK3 in intestinal epithelial cells, we expressed HA-SGK3 in Caco-2bbe cells stably expressing human NHE3V, Caco-2bbe/hNHE3V (Lin *et al.*, 2010). Dex treatment for 15 min stimulated NHE3 activity in HA-SGK3–expressing cells but not in pcDNA-transfected control cells (Figure 9A). Confocal

immunofluorescence analysis showed that SGK3 (green) colocalized with NHE3 (red) in the subapical compartments (Figure 9B). A cross-sectional view of the cells near the top surface and a stacked view show the apical expression of NHE3, which overlaps with fluorescent wheat germ agglutinin (WGA) that labels glycoprotein at the plasma membrane (Figure 9C, Cont). Treatment of the cells with Dex for 15 min enhanced the overlap of fluorescence labels of NHE3 and WGA, indicating increased surface NHE3 abundance in response to Dex (Figure 9C, Dex). The results from immunofluorescence analysis were confirmed by a surface biotinylation assay, which showed increased NHE3 protein abundance at the apical membrane (Figure 9D).

DISCUSSION

We have previously shown that SGK1 plays a critical role in Dex-induced activation of NHE3 in cultured fibroblast and epithelial cells (Yun *et al.*, 2002a; Wang *et al.*, 2005). However, the critical importance of SGK1 for NHE3 regulation in vivo has remained elusive until the recent report by Grahammer *et al.* (2006). In that study, the effects of Dex on intestinal NHE3 regulation were compared between WT and SGK1-null mice following a 4-d Dex treatment. Therefore we revisited Dex-induced regulation of NHE3 in the SGK1-null intestine to determine the effects at earlier time points at which NHE3 activity is increased but NHE3 abundance is not changed by Dex treatment. Moreover, we used mice with intestinal epithelia–specific deletion of SGK1. Our data showed that SGK1 plays a major role in short-term (4 h) regulation of NHE3 by Dex, and also confirmed the earlier report by Grahammer and coworkers. In addition, in agreement with our previous in vitro study that NHERF2 is required for SGK1-dependent regulation of NHE3, the NHERF2-null intestine showed decreased responses to Dex. However, the loss of neither SGK1 nor NHERF2 completely ablated the stimulatory effect of Dex. Our previous study showed that NHE3 abundance is not changed until much later than 4 h of Dex treatment and hence it is unlikely that the residual effect on NHE3 is simply due to changes in NHE3 abundance. Because SGKs share similar functions in regulation of various ion channels and transporters (Lang *et al.*, 2003, 2006), we determined whether SGK2 or SGK3 is involved in NHE3 regulation. Our current study using PS120 cells showed that both SGK2 and SGK3 activate NHE3. Our previous study has shown that SGK1, but not SGK2 and SGK3, interacts with NHERF2 (Yun *et al.*, 2002a). Consistently, stimulation of NHE3 activity by SGK2 and SGK3 was independent of NHERF2, occurring in PS120 cells that lack endogenous NHERF2, whereas SGK1 failed to regulate NHE3. A recent study showed that constitutively active SGK2, but not SGK1, stimulates NHE3 activity in OK cells (Pao *et al.*, 2010). This finding is consistent with previous studies that OK cells express NHERF2 at low levels (Yun *et al.*, 2002a). Apart from not needing NHERF2, all SGKs share common mechanisms that involve increased NHE3 abundance at 4 and 24 h of Dex treatment and the inability to regulate NHE3-S663A. In light of the high similarity of the kinase domains of SGK1–3, it is not surprising that they mediate Dex-induced activation of NHE3 via similar mechanisms. However, accumulating evidence shows that SGK3 plays distinct roles from SGK1. SGK3 is important for postnatal hair follicle growth (McCormick *et al.*, 2004), and a recent study showed that expression of SGK3 is estrogen-inducible in breast cancer cells (Wang *et al.*, 2011). In the current study, we showed for the first time that SGK3, but not SGK1 or SGK2, mediates an acute activation of NHE3 at as early as 15 min in response to Dex.

GC-mediated effects generally involve GR-dependent gene regulation. However, recent studies have highlighted short-term effects of GCs (Losel and Wehling, 2003), although the underlying mechanisms remain unclear. It was shown that Dex stimulates PI3K activity by potentiating binding of GR to the p85 subunit of PI3K (Hafezi-Moghadam *et al.*, 2002; Hu *et al.*, 2009). Unlike the classical activation of PI3K by insulin/IGF-1 receptors or tyrosine kinase receptors that occurs as a membrane-based event, GR-dependent activation of PI3K happens most likely in the cytoplasm with PI3K being sequestered away from the membrane (Hu *et al.*, 2009), which in turn activates PDK1. A previous study showed that all SGKs are phosphorylated by PDK1 (Kobayashi *et al.*, 1999), and knockdown of PDK1 abolished Dex-induced regulation of SGK2, SGK3, and NHE3 (Figures 8 and S4). We did not determine whether PDK1 directly regulates SGK1, but it was shown that PDK1 is required for PI3K-mediated activation of SGK1 and that SGK1-dependent activation of NHE3 involves PI3K (Park *et al.*, 1999; Yun *et al.*, 2002a). Hence it is highly likely that PDK1 links PI3K to SGK1.

So, what makes SGK3 different from other SGKs? We showed that SGK1 and SGK2 are diffusely distributed throughout the cytoplasm, with some in nuclei, but none on endosomes (Figure 6). On the other hand, SGK3 is distinctly localized to recycling and early endosomes, which is consistent with previous reports using HEK293 and COS cells (Jun *et al.*, 2001; Virbasius *et al.*, 2001; Tessier and Woodgett, 2006). On activation with Dex, p-PDK1 is recruited to endosomes, where it activates SGK3, as demonstrated by increased colocalization of p-PDK1 with SGK3 and Rab11 (Figures 8 and S6). In agreement with our findings, a recent study demonstrated that SGK3 facilitates the recruitment of p-PDK1 to endosomes when SGK3 is preactivated at S486 through PI3K signaling (Slagsvold *et al.*, 2006). Hence our current study demonstrates that the core of the acute regulation of SGK3 is its endosomal localization. The importance of endosomal residence of SGK3 for its regulation of NHE3 was further demonstrated by the finding that the R90A mutation in SGK3, which perturbed the endosomal localization of SGK3, lost its acute effect on NHE3 regulation, although delayed activation of NHE3 was not affected. How Dex induces delayed effects on NHE3 is not clear. We propose that SGK1 and SGK2, as well as the SGK3-R90A mutant deficient in the endosome-targeting PX domain, lack the spatial arrangement for a rapid access by PDK1 in response to Dex. Instead, much longer time is required for PDK1 and these SGKs to come in contact for activation of SGKs. In addition, cytosolic SGK1 and SGK2 may need to move through the cytoplasmic matrix to interact with and phosphorylate NHE3 (Figure 10).

Since the seminal studies by Grinstein and his colleagues in the late 1990s that showed NHE3 in recycling endosomes (D'Souza *et al.*, 1998; Kurashima *et al.*, 1998), the trafficking of NHE3 protein from recycling endosomes has been recognized as the pivotal step in NHE3 regulation. The former studies showed that inhibition of PI3K results in a pronounced loss of NHE3 from the cell surface and its accumulation in an intracellular endosomal compartment. Moreover, PI3K regulates NHE3 by several hormones and growth factors, including insulin, lysophosphatidic acid, and basic fibroblast growth factor (Janecki *et al.*, 2000; Lee-Kwon *et al.*, 2003; Fuster *et al.*, 2007). However, the identity of the effector(s) of PI3K signaling targeting NHE3 in recycling endosomes has remained undefined. Our present study is the first to identify SGK3 as a PI3K-signaling effector in recycling endosomes that activates NHE3. We therefore speculate that the endosomal localization of SGK3 has a broader implication on NHE3 regulation. In addition, the localization of SGK3 in recycling endosomes and the broad tissue expression of SGK3 suggest that SGK3, under basal or induced conditions, might be involved in regulating other proteins that traffic between intracellular pools and the plasma membrane.

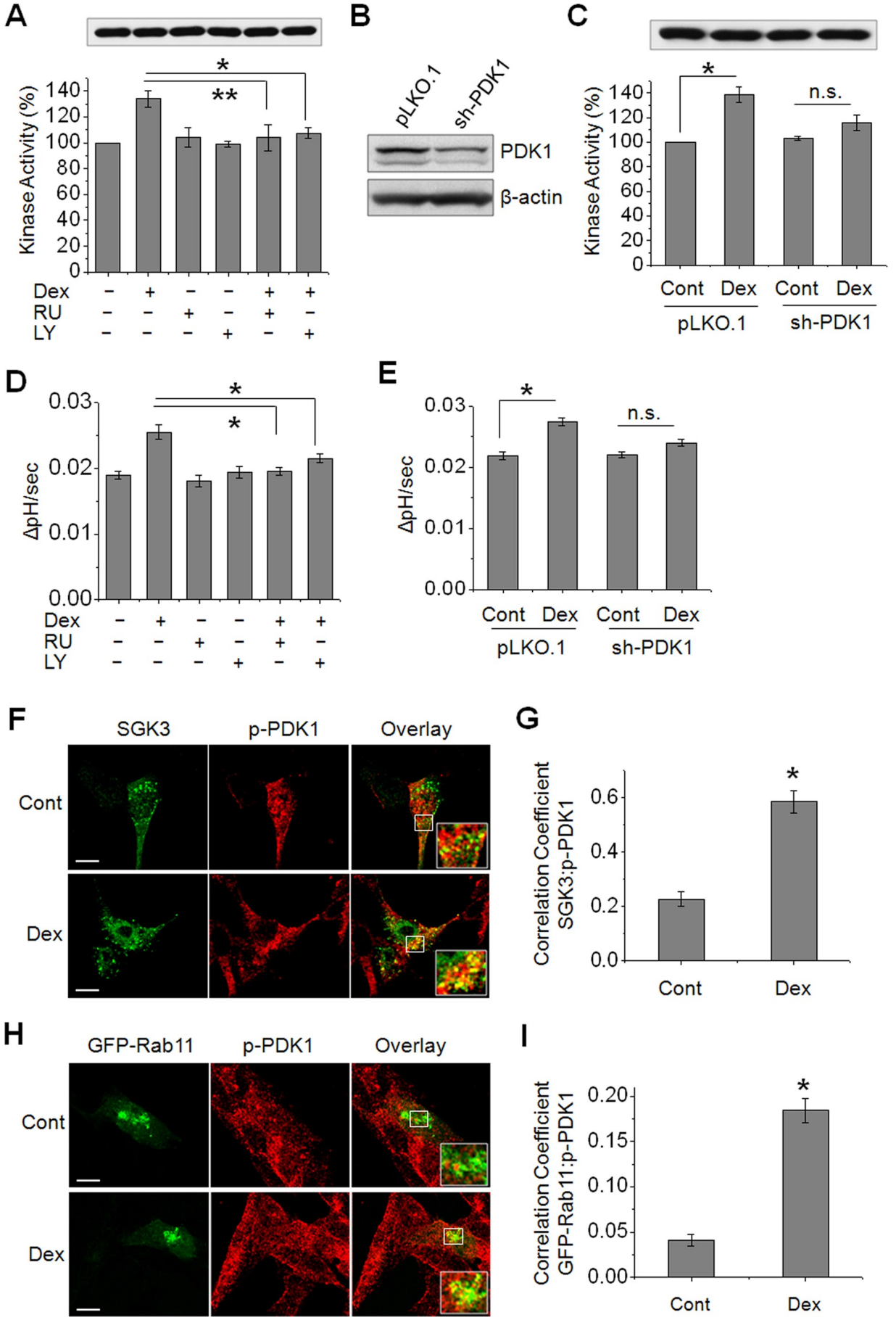
A
Kinase Activity (%)
140
120
100
80
60
40
20
0
*
**
Dex − + − − + +
RU − − + − + −
LY − − − + − +
B
pLKO.1
sh-PDK1
PDK1
β-actin
C
Kinase Activity (%)
*
n.s.
Cont Dex Cont Dex
pLKO.1 sh-PDK1
D
ΔpH/sec
0.03
0.02
0.01
0.00
*
*
Dex − + − − + +
RU − − + − + −
LY − − − + − +
E
ΔpH/sec
*
n.s.
Cont Dex Cont Dex
pLKO.1 sh-PDK1
F
SGK3
p-PDK1
Overlay
Cont
Dex
G
Correlation Coefficient SGK3:p-PDK1
0.6
0.4
0.2
0.0
*
Cont Dex
H
GFP-Rab11
p-PDK1
Overlay
Cont
Dex
I
Correlation Coefficient GFP-Rab11:p-PDK1
0.20
0.15
0.10
0.05
0.00
*
Cont Dex

In summary, our study showed that SGK1 plays a major role in Dex-mediated activation of NHE3 in vivo in the intestine, but some NHE3 activity regulation is independent of SGK1 and NHERF2. We showed that both SGK2 and SGK3 contribute to NHE3 activation, but SGK3 uniquely colocalizes with NHE3 to recycling endosomes, enabling acute regulation of NHE3 via the PI3K-PDK1 pathway.

MATERIALS AND METHODS

Animals

Generation of mice with the *sgk1* gene flanked by loxP (*Sgk1*$^{flox/flox}$) in C57BL/6 background was reported previously (Fejes-Toth *et al.*, 2008). Intestinal epithelia-specific deletion of SGK1 was achieved by mating *Sgk1*$^{flox/flox}$ mice with *Villin-Cre* transgenic mice. *Nherf2*-null (*Nherf2*$^{-/-}$) mice in C57BL/6 background have been previously described (Lin *et al.*, 2009). Genotypes were determined by PCR on tail DNA. In all experiments, age- and sex-matched littermates of *Sgk1*$^{flox/flox}$ and *Sgk1*$^{flox/flox}$*;Villin-Cre* or WT and *Nherf2*$^{-/-}$ mice were studied. Animals were maintained and experiments were performed under the institutional guidelines of Emory University.

Antibodies and plasmid constructs

Anti-HA, anti-PDK1, and anti–p-PDK1(Ser241) antibodies were purchased from Cell Signaling Technology (Danvers, MA). Anti-HA antibody was obtained from Covance (Denver, PA). Rabbit and mouse anti-FLAG antibodies were purchased from Sigma (St. Louis, MO) and anti-Rab5 antibody from Santa Cruz Biotechnology (Santa Cruz, CA). The pBK plasmid harboring HA-tagged human SGK1 has been previously described (Wang *et al.*, 2005). HA-tagged human SGK2 and SGK3 and FLAG-tagged SGK1 and SGK2 were cloned in pcDNA3.1-hygro. FLAG-SGK3 and pEGFP-Rab11 were obtained from Addgene (Cambridge, MA). The pLKO.1 plasmid harboring sh-PDK1 was purchased from Open Biosystems (Huntsville, AL). OKNHE3-S663A has been previously described (Wang *et al.*, 2005). SGK3-R90A was generated with the QuickChange II XL Site-Directed Mutagenesis Kit according to the recommendation by the manufacturer (Stratagene, Santa Clara, CA). The presence of mutation was confirmed by nucleotide sequencing.

Cell culture and transfection

PS120/NHE3V and PS120 expressing OKNHE3, PS120/OKNHE3, have been previously described (Wang *et al.*, 2005; He *et al.*, 2008). Caco-2bbe/hNHE3V cells were cultured as previously described (Lin *et al.*, 2010). Transfection was performed using the Neon Transfection System according to the manufacturer's recommendation (Invitrogen, Carlsbad, CA). Stable cell lines expressing SGK plasmids were selected with 800 μg/ml of neomycin or 600 μg/ml of hygromycin. Both PS120 fibroblasts and Caco-2bbe epithelial cells were cultured in DMEM supplemented with 1 mM sodium pyruvate, 50 U/ml penicillin, 50 μg/ml streptomycin, and 10% fetal bovine serum in a 5% CO_2 humidified incubator at 37°C.

Immunoprecipitation and kinase activity assay

PS120/NHE3V cells overexpressing HA-SGK1, HA-SGK2, HA-SGK3, or HA-SGK3-R90A were treated with 1 μM Dex. Cells were then lysed in lysis buffer containing 20 mM Tris-HCl (pH 7.5), 150 mM NaCl, 5 mM β-glycerophosphate, 2.5 mM sodium pyrophosphate, 1 mM Na_2EDTA, 1 mM ethylene glycol tetraacetic acid (EGTA), 1 mM Na_3VO_4, 1 mM sodium fluoride, 10 mM 1 μg/ml leupeptin, 1% Triton X-100, and protease inhibitor cocktail tablets (Roche, Indianapolis, IN). The crude lysate was sonicated twice for 15 s and spun at 14,000 × *g* for 15 min. Protein concentration was determined by the bicinchoninic acid assay (Sigma). Two milligrams of lysate was incubated overnight with or without anti-HA antibody. The immunocomplex was purified by incubation with 80 μl of protein A-Sepharose beads for 1 h, which was followed by three washes in lysis buffer and two washes in phosphate-buffered saline (PBS). Beads bound with SGK1, SGK2, SGK3, or SGK3-R90A were eluted with 50 μg/ml HA peptide (Covance) in elution buffer (50 mM Tris-HCl, pH 7.5, 150 mM NaCl, 270 mM sucrose, 1 mM Na_3VO_4, 0.1 mM EGTA, 0.2 mM phenylmethylsulfonyl fluoride, 0.1% β-mercaptoethanol and 10% glycerol). An aliquot of eluted protein was resolved by SDS–PAGE and immunoblotted with anti-HA antibody to ensure an identical amount of protein was used for kinase assay. In vitro kinase assay was determined with two approaches using 1) [γ-^{32}P]ATP and 2) a nonradioisotope TR-FRET method. For the former, the kinase assay was performed for 20 min at 30°C in 50 μl of reaction volume containing 10 μl of immunoprecipitate in reaction buffer (20 mM Tris, 100 μM ATP, 10 mM $MgCl_2$, 1 mM dithiothreitol [DTT], 10 μCi [γ-^{32}P]ATP) and 0.3 mM Crosstide (GRPRTSSFAEG; Upstate, Lake Placid, NY) as a substrate. The reaction was stopped with stop solution (1 mM ATP, 1% bovine serum albumin, and 0.6% HCl), and the reaction mix was applied to 2.1 cm p81 Whatman filter paper. After drying at room temperature, the filters were washed four times with 25 mM phosphoric acid and once with acetone and were then counted in a scintillation counter. For the latter nonradioisotope TR-FRET method, the assay was performed as previously reported in 384-well plates according to the manufacturer's recommendation (Zhang *et al.*, 2006). The same amount of eluted protein was incubated with ULight-PLK(Ser137) peptide (PerkinElmer, Waltham, MA) for 60 min at room temperature in kinase assay buffer (50 mM HEPES, pH 7.5, 1 mM EGTA, 10 mM $MgCl_2$, 2 mM DTT, and 0.01% Tween-20). The reaction was then stopped by addition of stop solution (detection

FIGURE 8: SGK3-mediated activation of NHE3 is dependent on PI3K and PDK1. (A) PS120/NHE3V/HA-SGK3 cells were pretreated with 1 μM RU or 20 μM LY prior to treatment with 1 μM Dex or carrier for 15 min. SGK3 protein was purified by immunoprecipitation, and the kinase activity was determined by TR-FRET. n = 3. (B) PS120/NHE3V/HA-SGK3 cells were stably transfected with sh-PDK1 or pLKO.1, and the expression level of PDK1 was determined by Western blotting using an anti-PDK1 antibody. (C) PS120/NHE3V/HA-SGK3 cells transfected with sh-PDK1 or pLKO.1 were treated with 1 μM Dex or carrier for 15 min. SGK3 protein was purified, and kinase activity was determined. n = 3. (D) NHE3 activities were determined in PS120/NHE3V/HA-SGK3 cells pretreated with RU or LY prior to treatment with Dex. (E) NHE3 activities in PS120/NHE3V/HA-SGK3 cells transfected with sh-PDK1 or pLKO.1 are shown. (A–E) n.s., not significant. *, $p < 0.01$ and **, $p < 0.05$, compared with respective controls. n = 6. (F) PS120/NHE3V cells expressing HA-SGK3 were serum-starved and treated with Dex or carrier for 15 min. Colocalization of SGK3 (green) and phospho-PDK1(p-PDK1, red) was determined using anti-HA and anti-p-PDK1 antibodies, respectively. (G) The graph represents Pearson's coefficient of SGK3 and p-PDK1 colocalization from 10 independent fields of cells. *, $p < 0.01$ compared with the control. (H) Colocalization of GFP-Rab11 (green) and p-PDK1 (red) in PS120/NHE3V cells treated with or without Dex for 15 min is shown. Scale bar: 10 μm. Insets show high magnification of merged signals. (I) Pearson's coefficient of GFP-Rab11 and p-PDK1 colocalization from 10 independent fields of cells. *, $p < 0.01$ compared with the control.

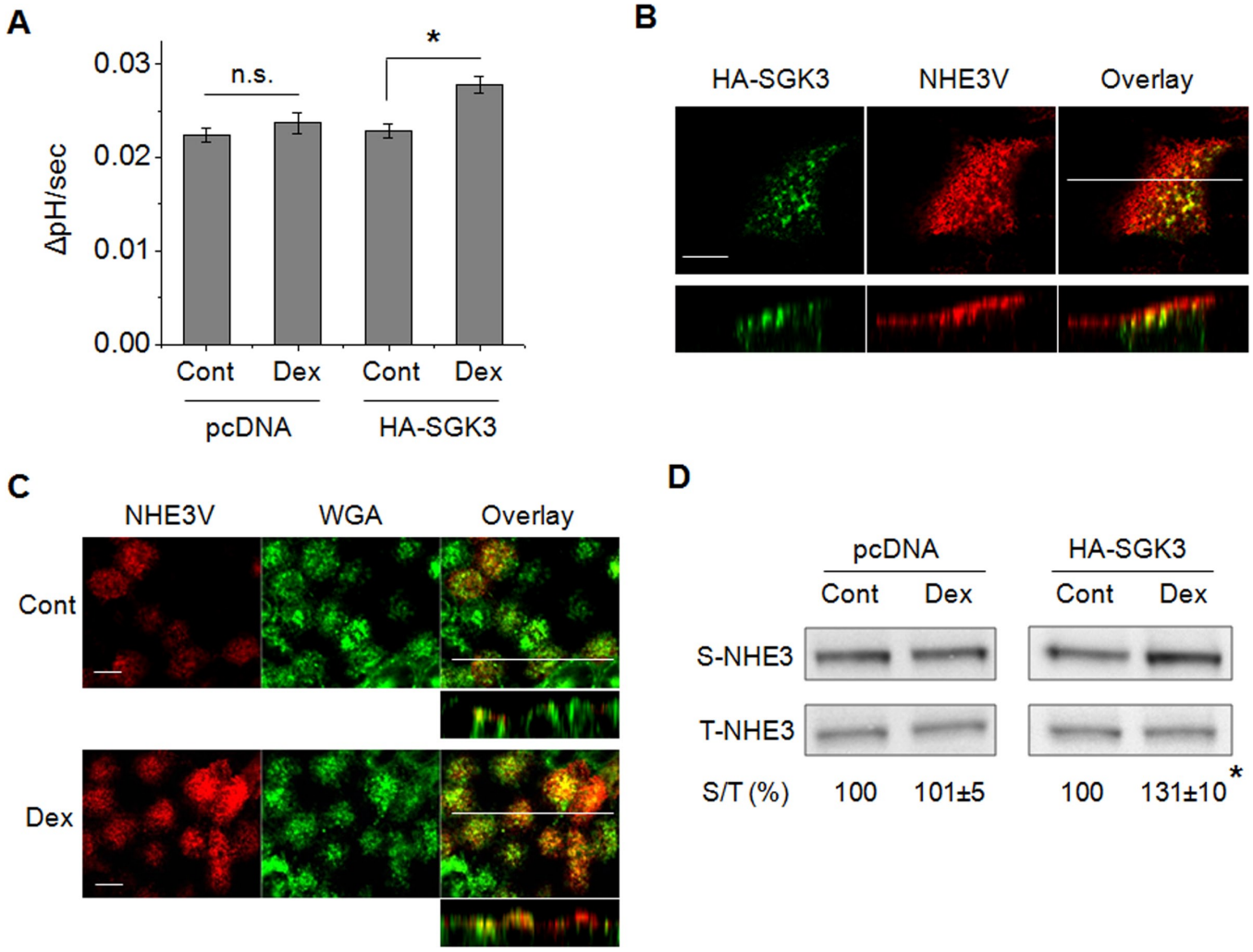

FIGURE 9: SGK3 mediates an acute activation of NHE3 by Dex in Caco-2bbe cells. (A) Caco-2bbe/hNHE3V/HA-SGK3 and Caco-2bbe/hNHE3V/pcDNA cells were treated with Dex or carrier for 15 min. NHE3 activities were measured in the presence of 50 μM Hoe-694. The rates of pH recovery at pH_i 6.7 are shown. n = 6. n.s., not significant. *, $p < 0.01$ compared with the untreated control. (B) Cellular localization of SGK3 (green) and NHE3 (red) in Caco-2bbe cells was determined by indirect immunofluorescence with anti-HA and anti-VSVG antibodies, respectively. Confocal focal planes (top) and cross-sections (bottom) are shown. Scale bar: 10 μm. (C) Caco-2bbe/hNHE3V/HA-SGK3 cells were treated with Dex or carrier for 15 min. NHE3 expression (red) at the apical membrane was determined with anti-VSVG antibody. WGA (green) staining of glycoprotein at plasma membrane is shown as a marker of apical labeling. Confocal focal (large panel) and cross-sectional (small panel) views are shown. Scale bar: 10 μm. (D) The amount of NHE3 protein on the plasma membrane was determined by surface biotinylation, as detailed in *Materials and Methods*. The amount of surface (S) NHE3 was normalized to total (T) NHE3, and relative changes (%) are shown below the blotting. n = 3. *, $p < 0.01$ compared with the untreated control.

buffer containing 40 mM EDTA) for 5 min, which was followed by application of detection mix (2 nM Europium-anti-phospho-PLK(Ser137) [PerkinElmer, Winooski, VT] in detection buffer) and incubation for 60 min at room temperature. The signal was determined with BioTek plate reader in a TR-FRET mode (emission at 665 nm, excitation at 320 nm) and recorded for calibration of enzyme activity.

Surface biotinylation

Surface biotinylation of NHE3 was performed as previously described (He *et al.*, 2010). Briefly, PS120/NHE3V cells were serum-starved for 4 h and Caco-2bbe/hNHE3V cells for 24 h prior to treatment with 1 μM Dex for indicated time periods (Figure 5A). Cells were rinsed twice in PBS and incubated for 10 min in borate buffer (154 mM NaCl, 7.2 mM KCl, 1.8 mM $CaCl_2$, and 10 mM H_3BO_3, pH 9.0). Cells were then incubated for 40 min with 0.5 mg/ml NHS-SS-biotin (Pierce) in borate buffer. Unbound NHS-SS-biotin was quenched with Tris buffer (20 mM Tris, 120 mM NaCl, pH 7.4). Cells were then rinsed with PBS, scraped, lysed in the lysis buffer described above, and sonicated twice for 15 s. The lysate was agitated for 30 min and spun at 14,000 × *g* for 30 min to remove the insoluble cell debris. An aliquot was retained as the total fraction representing the total cellular NHE3. Protein concentration was determined, and 1 mg of lysate was then incubated with streptavidin-agarose beads (Pierce) for 2 h. The strepavidin-agarose beads were washed three times in lysis buffer and twice in PBS. All the above procedures were performed at

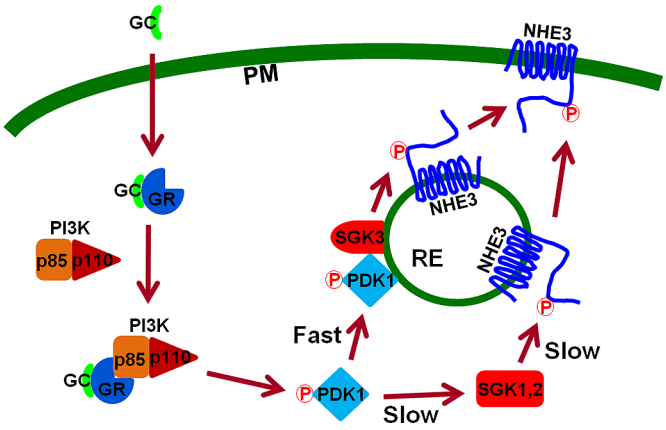

FIGURE 10: A schematic model of GC-mediated acute activation of NHE3 via SGK3. Previous studies showed that GCs bind to GR, and activated GR interacts with the p85 regulatory subunit of PI3K and recruits the p110 catalytic subunit in the cytoplasm (Hafezi-Moghadam *et al.*, 2002; Limbourg *et al.*, 2002; Hu *et al.*, 2009). PI3K activates PDK1 by phosphorylating PDK1, which acutely mobilizes to recycling endosomes (RE), where SGK3 and NHE3 are expressed. PDK1 then activates SGK3, which in turn phosphorylates NHE3 and induces exocytotic insertion of NHE3 into the plasma membrane (PM). This cascade occurs as part of the acute NHE3 activation by Dex involving SGK3. In the absence of SGK3, the activated PDK1 diffuses through cytoplasmic matrix and activates SGK1 or SGK2. Activated SGK1 and SGK2 then phosphorylate NHE3 at endosomes and potentiate trafficking of NHE3 to PM, a later pathway of NHE3 regulation.

4°C or on ice. Biotinylated surface proteins were then eluted by boiling the beads at 95°C for 10 min. Dilutions of the total and surface NHE3 were resolved by SDS–PAGE and immunoblotted with an anti-VSVG antibody. Densitometric analysis was performed using Scion Image software (www.nist.gov/lispix/imlab/prelim/dnld.html).

Na^+-dependent intracellular pH recovery

Mice were injected with Dex (2 mg/kg body weight) intraperitoneally, and the animals were killed 4 or 24 h later. Isolation of villi was performed as previously described (Grahammer *et al.*, 2006). In brief, mice were killed and the ileum was flushed with cold PBS to remove food particles. A segment of ileum ~10 cm from the cecum was always selected, opened longitudinally, and stabilized on a cooled stage. The villi were then carefully dissected under a stereomicroscope using sharpened microdissection scissors. Isolated villi were mounted on coverslips and covered with light- and solution-penetrable polycarbonate membrane (GE Healthcare, Minnetonka, MN). The intrinsic buffering capacity (IBC) of isolated villi was calibrated as previously described (Grahammer *et al.*, 2006) to confirm the IBC is similar between *Sgk1*$^{flox/flox}$ and *Sgk1*$^{flox/flox}$*;Villin-Cre* villi.

The Na^+-dependent changes in intracellular pH (pH_i) of isolated villi were determined with the use of the ratio-fluorometric (excitation: 495 and 440 nm, emission: 530 nm), pH-sensitive dye 2′,7′-bis-(2-carboxyethyl)-5-carboxyfluorescein acetoxymethyl ester (BCECF-AM; Sigma; Lamprecht *et al.*, 1998; He *et al.*, 2008). Briefly, villi were washed in Na^+ buffer (130 mM NaCl, 20 mM HEPES, 5 mM KCl, 1 mM tetramethylammonium-PO_4 [TMA-PO_4], 2 mM $CaCl_2$, 1 mM $MgSO_4$, and 25 mM glucose) and then were dye-loaded by incubating with 6.5 μM BCECF-AM in the same solution for 10 min. The coverslips were mounted on a perfusion chamber mounted on an inverted microscope and were superfused with NH_4^+ buffer (40 mM NH_4Cl, 90 mM NaCl, 20 mM HEPES, 5 mM KCl, 1 mM TMA-PO_4, 2 mM $CaCl_2$, 1 mM $MgSO_4$, and 25 mM glucose) and subsequently with TMA^+ buffer (130 mM TMA-Cl, 20 mM HEPES, 5 mM KCl, 1 mM TMA-PO_4, 2 mM $CaCl_2$, 1 mM $MgSO_4$, and 25 mM glucose). Na^+ buffer supplemented with 50 μM Hoe-694 (NHE1 and NHE2 inhibitor) or 10 μM S-3226 (NHE3 inhibitor) was then reintroduced to drive Na^+-dependent pH recovery. NHE3 activity in cultured cells was likewise determined. PS120 fibroblasts and Caco-2bbe cells seeded on coverslips were grown to 80–90% confluence and 5–7 d postconfluence, respectively. PS120 and Caco-2bbe cells were serum-starved for 4 h and overnight, respectively, prior to Dex treatment and NHE3 activity measurement. The rate of Na^+-dependent pH recovery was calculated by determining slopes along the early stage of pH recovery by linear least-squares analysis over a minimum of 9 s. Calibration of the fluorescence signal was performed using the K^+/H^+ ionophore nigericin as previously described (Lamprecht *et al.*, 1998). Comparisons of Na^+/H^+ exchange were made between measurements made on the same day. The microfluorometry was performed on a Nikon (Melville, NY) TE200 inverted microscope with a Nikon CFI Super Fluor 40× objective, coupled to a Lambda 10-2 filter wheel controller equipped with a multiwavelength filter set designed for BCECF-AM. Photometric data were acquired using MetaFluor software (Molecular Devices, Sunnyvale, CA).

Confocal immunofluorescence

PS120 cells grown on coverslips and Caco-2bbe cells grown on Transwell filters were fixed and permeabilized as described previously (He *et al.*, 2008). For labeling of glycoprotein as a marker of apical membrane, Caco-2bbe cells were subjected to 10-min incubation with Alexa Fluor 647-conjugated WGA (Invitrogen) prior to fixation. Cells were then stained with a rabbit monoclonal anti-HA antibody, a rabbit or mouse anti-FLAG antibody, a mouse monoclonal anti-VSVG antibody, a rabbit monoclonal anti–p-PDK1 antibody, or a mouse monoclonal anti-Rab5 antibody for 1 h at room temperature. Following three washes, 10 min each, with PBS, the cells were incubated with Alexa Fluor 488-conjugated goat anti–rabbit immunoglobulin G (IgG), Alexa Fluor 546-conjugated goat anti–rabbit IgG, Alexa Fluor 555-conjugated goat anti–mouse IgG, or Alexa Fluor 647–conjugated donkey anti–mouse IgG (Invitrogen) for 1 h at room temperature. After three 10-min washes with PBS, the specimens were mounted with ProLong Gold Antifade Reagent (Invitrogen) and observed under a Zeiss LSM510 laser confocal microscope (Zeiss Microimaging, Thornwood, NY) coupled to a Zeiss Axioplan2e with 60× Plan-Apochromat oil lenses. For quantitative evaluation of the colocalization of green (SGK3 or GFP-Rab11) and red (p-PDK1) fluorescence signals, 10 random fields of cells were selected. Pearson's correlation coefficient was determined for each cell using MetaMorph (Molecular Devices).

Statistical analysis

Results are presented as the mean ± SE. Statistical significance was assessed by Student's *t* test using the SPSS statistical program (SPSS, IBM, New York, NY). $p < 0.05$ is considered significant.

ACKNOWLEDGMENTS

This work was supported by grants from the National Institutes of Health (DK-061418 and DK-061418S1). P.H. and S.L. were supported by postdoctoral fellowships from the American Heart Association and Crohn's and Colitis Foundation of America, respectively. We acknowledge the Emory Digestive Disease Research Development Center (supported by DK-064399) for the use of its confocal

microscope. We thank Bing Yu and Nandan Mandayam in the laboratory of Vincent Yang at Emory University, Atlanta, GA, for helping with the MetaMorph software.

REFERENCES

Alvarez de la Rosa D, Zhang P, Naray-Fejes-Toth A, Fejes-Toth G, Canessa CM (1999). The serum and glucocorticoid kinase *sgk* increases the abundance of epithelial sodium channels in the plasma membrane of *Xenopus* oocytes. J Biol Chem 274, 37834–37839.

Baum M, Moe OW, Gentry DL, Alpern RJ (1994). Effect of glucocorticoids on renal cortical NHE-3 and NHE-1 mRNA. Am J Physiol 267, F437–E442.

Biemesderfer D, Rutherford PA, Nagy T, Pizzonia JH, AbuAlfa AK, Aronson PS (1997). Monoclonal antibodies for high-resolution localization of NHE3 in adult and neonatal rat kidney. Am J Physiol Renal Physiol 273, F289–F299.

Boehmer C, Henke G, Schniepp R, Palmada M, Rothstein JD, Broer S, Lang F (2003). Regulation of the glutamate transporter EAAT1 by the ubiquitin ligase Nedd4-2 and the serum and glucocorticoid-inducible kinase isoforms SGK1/3 and protein kinase B. J Neurochem 86, 1181–1188.

Bohmer C, Sopjani M, Klaus F, Lindner R, Laufer J, Jeyaraj S, Lang F, Palmada M (2010). The serum and glucocorticoid inducible kinases SGK1-3 stimulate the neutral amino acid transporter SLC6A19. Cell Physiol Biochem 25, 723–732.

Campieri M *et al.* (1997). Oral budesonide is as effective as oral prednisolone in active Crohn's disease. Gut 41, 209–214.

Charney AN, Kinsey MD, Myers L, Giannella RA, Gots RE (1975). Na^+-K^+-activated adenosine-triphosphatase and intestinal electrolyte transport—effect of adrenal steroids. J Clin Invest 56, 653–660.

D'Souza S, Garcia-Cabado A, Yu F, Teter K, Lukacs G, Skorecki K, Moore HP, Orlowski J, Grinstein S (1998). The epithelial sodium-hydrogen antiporter Na+/H+ exchanger 3 accumulates and is functional in recycling endosomes. J Biol Chem 273, 2035–2043.

Debonneville C *et al.* (2001). Phosphorylation of Nedd4-2 by Sgk1 regulates epithelial Na^+ channel cell surface expression. EMBO J 20, 7052–7059.

Embark HM, Bohmer C, Vallon V, Luft F, Lang F (2003). Regulation of KCNE1-dependent K^+ current by the serum and glucocorticoid-inducible kinase (SGK) isoforms. Pflugers Arch Eur J Physiol 445, 601–606.

Embark HM *et al.* (2004). Regulation of the epithelial Ca^{2+} channel TRPV5 by the NHE regulating factor NHERF2 and the serum and glucocorticoid inducible kinase isoforms SGK1 and SGK3 expressed in *Xenopus* oocytes. Cell Physiol Biochem 14, 203–212.

Fejes-Toth G, Frindt G, Naray-Fejes-Toth A, Palmer LG (2008). Epithelial Na^+ channel activation and processing in mice lacking SGK1. Am J Physiol Renal Physiol 294, F1298–F1305.

Friedrich B, Feng Y, Cohen P, Risler T, Vandewalle A, Broer S, Wang J, Pearce D, Lang F (2003). The serine/threonine kinases SGK2 and SGK3 are potent stimulators of the epithelial Na^+ channel α,β,γ-ENaC. Pflugers Arch Eur J Physiol 445, 693–696.

Fuster DG, Bobulescu IA, Zhang J, Wade J, Moe OW (2007). Characterization of the regulation of renal Na^+/H $^+$exchanger NHE3 by insulin. Am J Physiol Renal Physiol 292, F577–F585.

Gamper N, Fillon S, Huber SM, Feng Y, Kobayashi T, Cohen P, Lang F (2002). IGF-1 up-regulates K^+ channels via PI3-kinase, PDK1 and SGK1. Pflugers Arch Eur J Physiol 443, 625–634.

Grahammer F *et al.* (2006). Intestinal function of gene-targeted mice lacking serum- and glucocorticoid-inducible kinase 1. Am J Physiol Gastr L 290, G1114–G1123.

Hafezi-Moghadam A *et al.* (2002). Acute cardiovascular protective effects of corticosteroids are mediated by non-transcriptional activation of endothelial nitric oxide synthase. Nat Med 8, 473–479.

He PJ, Klein J, Yun CC (2010). Activation of Na^+/H^+ exchanger NHE3 by angiotensin II is mediated by inositol 1,4,5-triphosphate (IP3) receptor-binding protein released with IP3 (IRBIT) and Ca^{2+}/calmodulin-dependent protein kinase II. J Biol Chem 285, 27869–27878.

He PJ, Yun CC (2010). Mechanisms of the regulation of the intestinal Na^+/H^+ exchanger NHE3. J Biomed Biotechnol 2010, 238080.

He PJ, Zhang HC, Yun CC (2008). IRBIT, inositol 1,4,5-triphosphate (IP3) receptor-binding protein released with IP3, binds Na^+/H^+ exchanger NHE3 and activates NHE3 activity in response to calcium. J Biol Chem 283, 33544–33553.

Helms MN, Fejes-Toth G, Naray-Fejes-Toth A (2003). Hormone-regulated transepithelial Na^+ transport in mammalian CCD cells requires SGK1 expression. Am J Physiol Renal Physiol 284, F480–F487.

Henke G, Setiawan I, Bohmer C, Lang F (2002). Activation of Na^+/K^+-ATPase by the serum and glucocorticoid-dependent kinase isoforms. Kidney Blood Press Res 25, 370–374.

Hu Z, Wang H, Lee IH, Du J, Mitch WE (2009). Endogenous glucocorticoids and impaired insulin signaling are both required to stimulate muscle wasting under pathophysiological conditions in mice. J Clin Invest 119, 3059–3069.

Janecki AJ, Janecki M, Akhter S, Donowitz M (2000). Basic fibroblast growth factor stimulates surface expression and activity of Na(+)/H(+) exchanger NHE3 via mechanism involving phosphatidylinositol 3-kinase. J Biol Chem 275, 8133–8142.

Jun X, Liu D, Gill G, Zhou SY (2001). Regulation of cytokine-independent survival kinase (CISK) by the Phox homology domain and phosphoinositides. J Cell Biol 154, 699–705.

Kobayashi T, Deak M, Morrice N, Cohen P (1999). Characterization of the structure and regulation of two novel isoforms of serum- and glucocorticoid-induced protein kinase. Biochem J 344, 189–197.

Kurashima K, Szabo EZ, Lukacs G, Orlowski J, Grinstein S (1998). Endosomal recycling of the Na^+/H^+ exchanger NHE3 isoform is regulated by the phosphatidylinositol 3-kinase pathway. J Biol Chem 273, 20828–20836.

Lamprecht G, Weinman EJ, Yun CHC (1998). The role of NHERF and E3KARP in the cAMP-mediated inhibition of NHE3. J Biol Chem 273, 29972–29978.

Lang F, Bohmer C, Palmada M, Seebohm G, Strutz-Seebohm N, Vallon V (2006). (Patho)physiological significance of the serum- and glucocorticoid-inducible kinase isoforms. Physiol Rev 86, 1151–1178.

Lang F, Henke G, Embark HM, Waldegger W, Palmada M, Bohmer C, Vallon V (2003). Regulation of channels by the serum and glucocorticoid-inducible kinase-implications for transport, excitability and cell proliferation. Cell Physiol Biochem 13, 41–50.

Lee-Kwon W, Kawano K, Choi JW, Kim JH, Donowitz M (2003). Lysophosphatidic acid stimulates brush border Na^+/H^+ exchanger 3 (NHE3) activity by increasing its exocytosis by an NHE3 kinase A regulatory protein-dependent mechanism. J Biol Chem 278, 16494–16501.

Limbourg FP, Huang Z, Plumier JC, Simoncini T, Fujioka M, Tuckermann J, Schulz G, Moskowiz MA, Liao JK (2002). Rapid nontranscriptional activation of endothelial nitric oxide synthase mediates increased cerebral blood flow and stroke protection by corticosteroids. J Clin Invest 110, 1729–1738.

Lin SB, Wang DS, Iyer S, Ghaleb AM, Shim H, Yang VW, Chun J, Yun CC (2009). The absence of LPA(2) attenuates tumor formation in an experimental model of colitis-associated cancer. Gastroenterology 136, 1711–1720.

Lin SB *et al.* (2010). Lysophosphatidic acid stimulates the intestinal brush border Na^+/H^+ exchanger 3 and fluid absorption via LPA(5) and NHERF2. Gastroenterology 138, 649–658.

Losel R, Wehling M (2003). Nongenomic actions of steroid hormones. Nat Rev Mol Cell Biol 4, 46–56.

Maier C, Runzler D, Schindelar J, Grabner G, Waldhausl W, Kohler G, Luger A (2005). G-protein-coupled glucocorticoid receptors on the pituitary cell membrane. J Cell Sci 118, 3353–3361.

Maier G, Palmada M, Rajamanickam J, Shumilina E, Bohmer C, Lang F (2006). Upregulation of HERG channels by the serum and glucocorticoid inducible kinase isoform SGK3. Cell Physiol Biochem 18, 177–186.

McCormick JA *et al.* (2004). Targeted disruption of the protein kinase SGK3/CISK impairs postnatal hair follicle development. Mol Biol Cell 15, 4278–4288.

Naray-Fejes-Toth A, Canessa C, Cleaveland ES, Aldrich G, Fejes-Toth G (1999). *sgk* is an aldosterone-induced kinase in the renal collecting duct-Effects on epithelial Na^+ channels. J Biol Chem 274, 16973–16978.

Pao AC *et al.* (2010). Expression and role of serum and glucocorticoid-regulated kinase 2 in the regulation of Na^+/H^+ exchanger 3 in the mammalian kidney. Am J Physiol Renal Physiol 299, F1496–F1506.

Park J, Leong MLL, Buse P, Maiyar AC, Firestone GL, Hemmings BA (1999). Serum and glucocorticoid-inducible kinase (SGK) is a target of the PI 3-kinase-stimulated signaling pathway. EMBO J 18, 3024–3033.

Pinto D, Robine S, Jaisser F, El Marjou FE, Louvard D (1999). Regulatory sequences of the mouse villin gene that efficiently drive transgenic expression in immature and differentiated epithelial cells of small and large intestines. J Biol Chem 274, 6476–6482.

Ponting CP (1996). Novel domains in NADPH oxidase subunits, sorting nexins, and PtdIns 3-kinases: binding partners of SH3 domains? Protein Sci 5, 2353–2357.

Slagsvold T, Marchese A, Brech A, Stenmark H (2006). CISK attenuates degradation of the chemokine receptor CXCR4 via the ubiquitin ligase AIP4. EMBO J 25, 3738–3749.

Strutz-Seebohm N *et al*. (2005a). Regulation of GluR1 abundance in murine hippocampal neurones by serum- and glucocorticoid-inducible kinase 3. J Physiol 565, 381–390.
Strutz-Seebohm N *et al*. (2005b). Glucocorticoid adrenal steroids and glucocorticoid-inducible kinase isoforms in the regulation of GluR6 expression. J Physiol 565, 391–401.
Tessier M, Woodgett JR (2006). Role of the Phox homology domain and phosphorylation in activation of serum and glucocorticoid-regulated kinase-3. J Biol Chem 281, 23978–23989.
Virbasius JV, Song X, Pomerleau DP, Zhan Y, Zhou GW, Czech MP (2001). Activation of the Akt-related cytokine-independent survival kinase requires interaction of its phox domain with endosomal phosphatidylinositol 3-phosphate. Proc Natl Acad Sci USA 98, 12908–12913.
Wang DS, Sun H, Lang F, Yun CC (2005). Activation of NHE3 by dexamethasone requires phosphorylation of NHE3 at Ser663 by SGK1. Am J Physiol Cell Physiol 289, C802–C810.
Wang DS, Zhang HC, Lang F, Yun CC (2007). Acute activation of NHE3 by dexamethasone correlates with activation of SGK1 and requires a functional glucocorticoid receptor. Am J Physiol Cell Physiol 292, C396–C404.
Wang Y, Zhou D, Phung S, Masri S, Smith D, Chen S (2011). SGK3 is an estrogen-inducible kinase promoting estrogen-mediated survival of breast cancer cells. Mol Endocrinol 25, 72–82.
Webster MK, Goya L, Ge Y, Maiyar AC, Firestone GL (1993). Characterization of sgk, a novel member of the serine threonine protein-kinase gene family which is transcriptionally induced by glucocorticoids and serum. Mol Cell Biol 13, 2031–2040.
Worby CA, Dixon JE (2002). Sorting out the cellular functions of sorting nexins. Nature Rev Mol Cell Biol 3, 919–931.
Wulff P *et al*. (2002). Impaired renal Na^+ retention in the sgk1-knockout mouse. J Clin Invest 110, 1263–1268.
Yun CC, Chen YP, Lang F (2002a). Glucocorticoid activation of Na^+/H^+ exchanger isoform 3 revisited—the roles of SGK1 and NHERF2. J Biol Chem 277, 7676–7683.
Yun CC *et al*. (2002b). The serum and glucocorticoid-inducible kinase SGK1 and the Na^+/H^+ exchange regulating factor NHERF2 synergize to stimulate the renal outer medullary K^+ channel ROMK1. J Am Soc Nephrol 13, 2823–2830.
Yun CHC, Gurubhagavatula S, Levine SA, Montgomery JLM, Brant SR, Cohen ME, Cragoe EJ, Pouyssegur J, Tse CM, Donowitz M (1993). Glucocorticoid stimulation of ileal Na^+ absorptive cell brush-border Na^+ H^+ exchange and association with an increase in message for Nhe-3, an epithelial Na^+ H^+ exchanger isoform. J Biol Chem 268, 206–211.
Zhang WG, Shor B, Yu K (2006). Identification and characterization of a constitutively T-loop phosphorylated and active recombinant S6K1: expression, purification, and enzymatic studies in a high capacity non-radioactive TR-FRET Lance assay. Protein Expr Purif 46, 414–420.